Timing and Power Models for CMOS Repeaters Driving Resistive Interconnect

Victor Adler and Eby G. Friedman

Department of Electrical Engineering
University of Rochester
Rochester, NY 14627

adler@ee.rochester.edu, friedman@ee.rochester.edu

Abstract – A delay and power model of a CMOS inverting repeater driving a resistive-capacitive load is presented. The model is derived from Sakurai's alpha-power law and exhibits good accuracy. The model can be used to design and analyze those CMOS inverters that drive a large *RC* load when considering both speed and power. Expressions are provided for estimating the propagation delay and transition time and exhibit less than 27% discrepancy from SPICE for a wide variety of *RC* loads. Expressions are also provided for modeling the short-circuit power dissipation of a CMOS inverter driving a resistive-capacitive interconnect line which are accurate to within 15% of SPICE for most practical loads.

I. Introduction

As the die size of CMOS integrated circuits continues to increase, interconnections have become increasingly significant. With a linear increase in length, interconnect delay increases quadratically due to a linear increase in both interconnect resistance and capacitance [1]. Large interconnect loads not only affect performance but also cause excess power to be dissipated. A large *RC* load degrades the waveform shape, dissipating excessive short-circuit power in the following stages loading a CMOS logic gate.

Several methods have been introduced to reduce interconnect delay so that these impedances do not dominate the delay of a critical path [1–4]. Furthermore, with the introduction of portable computers, power has become an increasingly important factor in the circuit design process. Thus, power consumption must be accurately estimated when considering techniques for improving circuit speed when driving long interconnections. Therefore, circuit level models describing both dynamic power and, recently, short-circuit power have become increasingly important [5–8].

In this paper, an analytical expression for the transient response of a CMOS inverter driving a lumped *RC* load is presented. This approach is different from Kayssi *et al.* [9] in that a lumped *RC* load is considered rather than a lossless capacitive load. Furthermore, Sakurai's alpha-power law [10] is used to describe the circuit operation of the CMOS transistors rather than the classical Shichman-Hodges model [11]. The alpha-power law model considers short channel behavior, permitting increased accuracy and generality in the delay and power expressions. These expressions are used to estimate the propagation delay and the rise and fall times (or transition times) of a CMOS inverter. Since the output waveform is accurately calculated, the short-circuit

power [12] dissipated by the following stage can also be estimated. Furthermore, due to its relative simplicity, these expressions permit linear programming techniques to be used when optimizing the placement of buffers for both speed and power.

The paper is organized as follows: expressions for an inverter driving a lumped *RC* load are derived, and characteristic delay equations are presented and compared with SPICE in Section II. In Section III, an expression describing the short-circuit power dissipation of a CMOS inverter following a lumped *RC* load is introduced and compared with SPICE. Finally, some concluding remarks are offered in Section IV.

II. Analysis of an RC Loaded CMOS Inverter

An analytical expression describing the behavior of an inverter driving a lumped *RC* load based on Sakurai's alpha-power law model [10] is presented. A diagram of this circuit is shown in Figure 1.
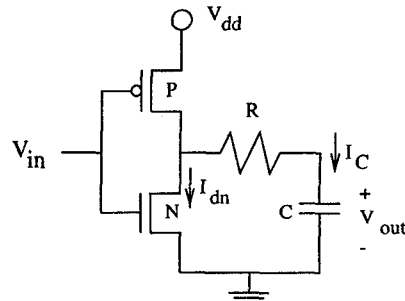

Figure 1. A CMOS inverter driving an *RC* load

The alpha-power law model [10] accurately describes the effects of short channel behavior, such as velocity saturation, while providing a tractable equation. The linear region form of the alpha-power model is used to characterize the I-V behavior of the ON transistor since a large portion of the circuit operation occurs within this region under the assumption of a step or fast ramp input signal.

Only the falling output (rising input) waveform is considered in this paper. The following analysis, however, is equally applicable to a rising output (falling input) waveform. The lumped load is modeled as a resistor in series with a capacitor. The current through the output load capacitance is the same magnitude and opposite sign as the N-channel drain current (the P-channel current is ignored under the assumption of a step or fast ramp input).

The N-channel linear drain current is given by [10]

$$-C\frac{dV_{out}}{dt} = i_d = \frac{I_{do}}{V_{do}}\left(\frac{V_{GS} - V_{T-}}{V_{DD} - V_T}\right)^\alpha V_{ds}, \quad (1)$$

$$for \ V_{GS} \geq V_T, V_{GS} - V_T \geq V_{DS}$$

where C is the output capacitance, V_{out} is the voltage across the capacitance C, and i_d is the drain current through the N-channel device.

In the alpha-power law model, I_{do} represents the drive current of the MOS device and is proportional to W/L, V_{do} represents the drain-to-source voltage at which velocity saturation occurs with $V_{GS} = V_{DD}$ and is a process dependent constant, and α models the process dependent degree to which velocity saturation affects the drain-to-source current. α is within the range $1 \le \alpha \le 2$, where $\alpha = 1$ corresponds to a device operating strongly under velocity saturation, while $\alpha = 2$ represents a device with negligible velocity saturation. V_{DD} is the supply voltage, and V_T is the MOS threshold voltage (where V_{TN} (V_{TP}) is the N-channel (P-channel) threshold voltage).

Assuming a unit step input is applied to the circuit shown in Figure 1, V_{out} can be derived from (1) and is

$$V_{out}(t) = V_{out}(0)e^{\frac{-\mho_{do}}{\mho_{do}RC+C}t} \quad , \qquad (2)$$

where $\mho_{do} = \frac{I_{do}}{V_{do}}$ is the saturation conductance [8]. Graphs of $V_{out}(t)$ for a wide range of resistive and capacitive values (within practical limits) are shown in Figure 2. The analytical expression shown in (2) closely approximates SPICE (within 25%) for most of the region of operation for a wide range of load impedances from 10 Ω to 1000 Ω and from 10 fF to 1 pF.
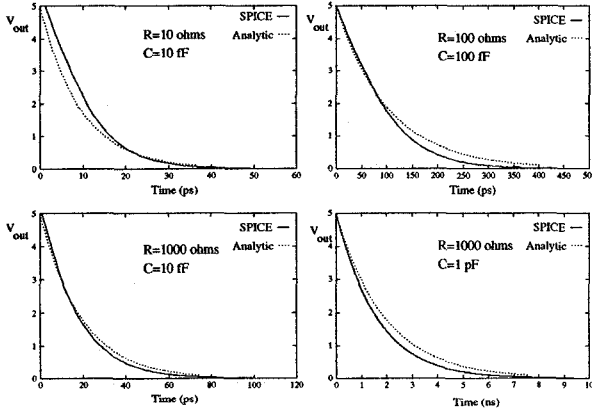

Figure 2. Output response of a CMOS inverter driving an RC load

From (2), the propagation delay of a CMOS inverter calculated at the 50% point t_{PD} is

$$t_{PD} = .693\frac{C + \mho_{do}RC}{\mho_{do}} \quad . \qquad (3)$$

The transition time of a CMOS inverter driving a lumped RC load calculated at the 90% point t_t is

$$t_t = 2.3\frac{C + \mho_{do}RC}{\mho_{do}} \quad . \qquad (4)$$

Additional delay expressions that are used in section III for determining the short-circuit power are

$$t_{V_{TN}} = \ln\left(\frac{V_{TN}}{V_{DD}}\right)\frac{C + \mho_{do}RC}{\mho_{do}} \qquad (5)$$

and

$$t_{V_{TP}} = \ln\left(\frac{V_{DD} + V_{TP}}{V_{DD}}\right)\frac{C + \mho_{do}RC}{\mho_{do}} \quad . \qquad (6)$$

These equations describe the time for the output voltage to change by a threshold voltage from either ground or V_{DD} for an N-channel or P-channel device, respectively. Note that V_{TP} is negative.

The accuracy of the analytic model as compared with SPICE is tabulated in Table I for a wide variety of output load resistances and capacitances, assuming a 0.8 μm CMOS technology. Note that the maximum error of the transition time t_t as compared with SPICE is 27%, and the maximum error of the propagation delay t_{PD} as compared with SPICE is 25%. As the load capacitance increases to 1 pF, the error of the propagation delay generally decreases to less than 20%. A similar decrease occurs for the transition time. Furthermore, both errors generally decrease with increasing load resistance.

Table I. Propagation delay t_{PD} and transition time t_t of an inverter driving an RC load (0.8 μm CMOS technology)

R	C	t_t		t_{PD}		% Error	
		Analytic	SPICE	Analytic	SPICE	t_t	t_{PD}
10 Ω	.01 pF	21 ps	22 ps	6.5 ps	8.7 ps	4%	25%
10 Ω	.1 pF	215 ps	176 ps	65 ps	70 ps	22%	7%
10 Ω	1 pF	2.2 ns	1.7 ns	649 ps	680 ps	27%	4%
100 Ω	.01 pF	24 ps	22 ps	7.2 ps	8.8 ps	6%	19%
100 Ω	.1 pF	235 ps	187 ps	71 ps	73 ps	25%	2 %
100 Ω	1 pF	2.4 ns	1.9 ns	712 ps	711 ps	25%	0 %
1000 Ω	.01 pF	44 ps	39 ps	13 ps	13 ps	13%	0 %
1000 Ω	.1 pF	444 ps	365 ps	133 ps	115 ps	22%	16%
1000 Ω	1 pF	4.4 ns	3.6 ns	1.3 ns	1.1 ns	22%	18%

The improved accuracy with increasing load resistance and capacitance is due to the RC load dominating the device parasitics, specifically, the source and drain capacitance, thereby improving the accuracy of the transistor I-V model for large RC loads. These device parasitic impedances are not included in the I-V model described in (1) but are considered by SPICE. This behavior also explains why the accuracy improves as the geometric size of the transistors becomes smaller, making the parasitic device resistances and capacitances smaller. Thus, these expressions for the propagation delay and transition time of a CMOS inverter driving an RC load become more accurate for higher RC loads and more aggressive submicrometer technologies, the regime of greatest interest.

III. Power Estimation

Power consumption has become one of the premier issues in VLSI circuit design. There are two primary contributions to the total transient power dissipated by a CMOS inverter, dynamic power dissipation and short-circuit power dissipation [5–8,12,13]. The short-circuit power is often neglected since the dynamic power is assumed to be dominant. As described below and in [5–8,12,13], the magnitude of the short-circuit power is load dependent and is shown in this paper to be a significant portion of the total dissipated power.

Dynamic power is due to the energy required to charge and discharge a load capacitance C and is characterized by the familiar equation, CV^2f, where V is the source voltage and f is the switching frequency. The dynamic

power is independent of the load resistance. For example, the dynamic power dissipation of a single CMOS inverter driving an RC load ranges from 35 μW to 125 μW for capacitive loads ranging from 0.3 pF to 1 pF, assuming a 5 volt power supply with the inverter switching every 10 MHz.

The logic stage following a large RC load may dissipate significant amounts of short-circuit power due to the degraded waveform originating from the CMOS inverter driving an RC load (see Figure 3). During the region where the input signal is transitioning between V_{TN} and $V_{DD}+V_{TP}$, a DC current path exists between V_{DD} and ground. The excess current dissipated during this region is called the short-circuit (or crossover) current [12]. Short-circuit current occurs due to a slow input transition, and for a balanced inverter, the peak current occurs near the middle of the input transition. An example of short-circuit current is shown by the solid line in the lower graph of Figure 4, *i.e.*, the SPICE-derived data.
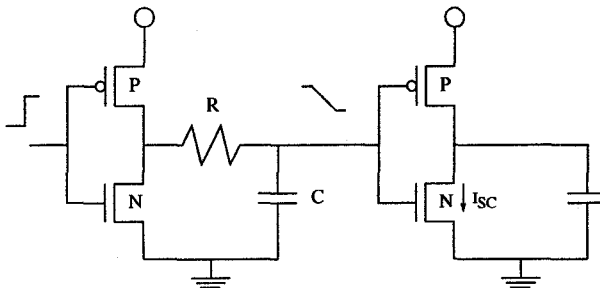

Figure 3. Non-step input driving CMOS inverter stage creates short-circuit power

The total short-circuit current I_{SC} can be estimated by modeling I_{SC} as a triangle. Therefore, the integral of I_{SC} is the area of a triangle, $\frac{1}{2}base \times height$. In terms of the short-circuit current, the height can be modeled as I_{peak} and the base can be modeled as t_{base} (see Figure 4). I_{peak} is the maximum saturation current of the load transistor and depends on both V_{GS} and V_{DS}, therefore I_{peak} is both input waveform and load dependent. t_{base} is the time during which the DC current path exists when both the P-channel and the N-channel transistors are turned on. This time occurs over the region, $V_{TN} \leq V_{in} \leq V_{DD} +V_{TP}$. Therefore, t_{base} is found from the difference between (5) and (6), $\left| \left(t_{V_{TP}} - t_{V_{TN}} \right) \right|$. The area defined by this triangle is $\frac{1}{2}I_{peak} \times t_{base}$, which models the total short-circuit current I_{SC} sourced by a CMOS inverter due to a non-step input.

The total short-circuit current multiplied by f and V_{DD} is the short-circuit power. The short-circuit power dissipation P_{SC} of the following stage for one transition (either rising or falling edge) can therefore be approximated by

$$ P_{SC} = \frac{1}{2}I_{peak}\, t_{base}\, V_{DD}\, f \quad . \tag{7} $$

Subtracting (5) from (6) forms the logarithmic quotient, $t_{base} = \left| \ln\left(\frac{V_{TN}}{V_{DD}+V_{TP}} \right) \right| \frac{C+\mho_{do}RC}{\mho_{do}}$. By inserting this expression for t_{base} into (7), the short-circuit power dissipation P_{SC} of a CMOS inverter following a lumped RC load over both the rising and falling transitions is

$$ P_{SC} = \left| \ln\left(\frac{V_{TN}}{V_{DD}+V_{TP}} \right) \right| \frac{C+\mho_{do}RC}{\mho_{do}} I_{peak} f V_{DD} \quad . \tag{8} $$
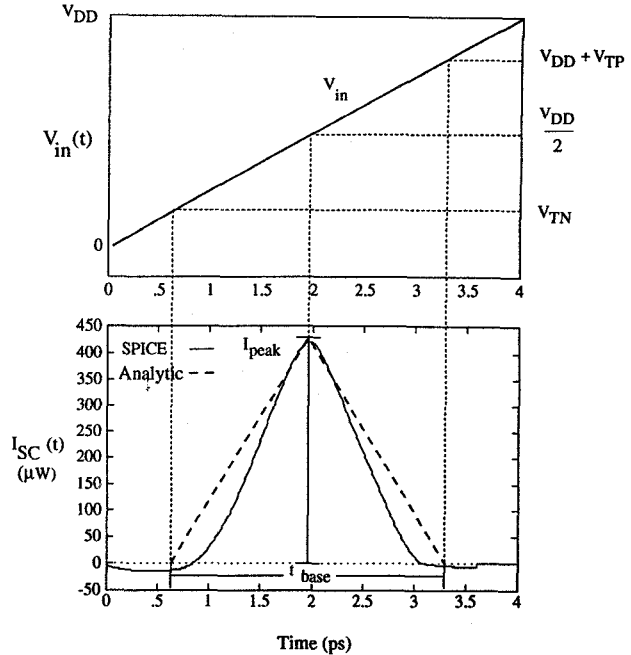

Figure 4. Graphical estimation of short-circuit current (0.8 μm CMOS technology)

The short-circuit power derived from (8) for a wide variety of RC loads between the CMOS inverter stages shown in Figure 3 is compared with SPICE in Table II.

Table II. Estimate of short-circuit power dissipated by a CMOS inverter (0.8 μm CMOS technology)

R	C	Power (μW) f = 10 MHz, V_{DD} = 5.0 V		% Error
		Analytic	SPICE	
10 Ω	.3 pF	1.4	.99	41%
10 Ω	.5 pF	3.9	3.22	21%
10 Ω	1 pF	12.4	11.1	12%
100 Ω	.3 pF	1.71	1.23	39%
100 Ω	.5 pF	4.68	3.83	22%
100 Ω	1 pF	13.8	12.7	9%
1000 Ω	.3 pF	5.85	5.2	12%
1000 Ω	.5 pF	13.0	12.2	7%
1000 Ω	1 pF	34.2	33.8	1%

For smaller RC loads, hence, faster transition times, there is negligible short-circuit power since a direct path from the power supply to ground does not exist for any significant time. The short-circuit power becomes non-negligible when larger interconnect loads between the two CMOS stages cause a transition time of significant magnitude (*e.g.*, $t_t > 0.5$ ns for a 0.8 μm CMOS inverter). At this borderline value, the analytical P_{SC} differs from SPICE by a maximum of 41%. As the RC load and transition time increase, the analytical model more closely predicts the short-circuit current derived from SPICE. For RC loads exceeding 0.1 ns, errors less than 15% are attained. Furthermore, the short-circuit power becomes a significant portion

203

of the total power dissipation when the CMOS inverter is loaded by larger RC loads, creating long transition times. It is this condition that is of greatest interest when considering short-circuit power in resistively loaded CMOS inverters.

The error of the analytical expression for P_{SC} can be bounded by the RC time constant describing the interconnect load impedance. For a 0.8 μm CMOS technology, the per cent error is less than 15% for an RC time constant more than 0.1 ns. For an RC time constant less than 0.1 ns, the error increases to approximately 40%.

For a given supply voltage and frequency, dynamic power dissipation depends only on the load capacitance and does not depend on the input waveform shape or load resistance. In contrast, the short-circuit power dissipation changes with both input waveform shape and output load resistance and capacitance. The ratio of the short-circuit power to the total transient power (the sum of the dynamic and short-circuit power) of a CMOS inverter with respect to the load resistance R for a given load capacitance C is shown in Figure 5. Note that with increasing load resistance, the short-circuit power cannot be neglected, since, as shown in Figure 5, it can comprise more than 20% of the total transient power dissipation.
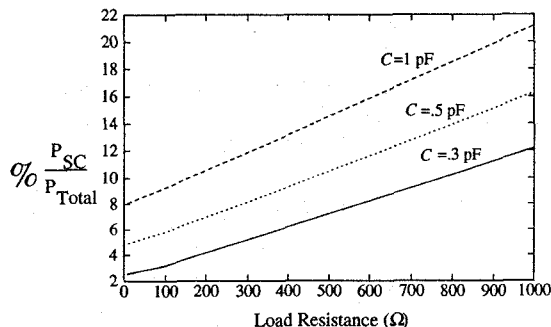

Figure 5. Ratio of short-circuit power to total transient power versus load resistance for varying load capacitance

IV. Conclusions

A simple yet accurate expression for the output voltage of a CMOS inverter as a function of time driving a resistive-capacitive load is presented. With this expression, equations characterizing the propagation delay and transition time of a CMOS inverter driving an RC load are presented. These expressions are accurate to within 25% of SPICE for a wide range of RC loads. Furthermore, since the output waveform of this circuit is accurately modeled, the short-circuit power dissipation of the following CMOS stage loading the interconnect line can be accurately estimated to within 15% for highly resistive loads. Therefore, due to the simplicity and accuracy of these expressions, the delay and power characteristics of a CMOS inverter driving a high impedance RC interconnect line can be efficiently estimated.

References

[1] H. B. Bakoglu and J. D. Meindl, "Optimal Interconnection Circuits for VLSI," *IEEE Transactions on Electron Devices*, Vol. ED-32, No. 5, pp. 903–909, May 1985.

[2] S. Dhar and M. A. Franklin, "Optimum Buffer Circuits for Driving Long Uniform Lines," *IEEE Journal of Solid-State Circuits*, Vol. SC-26, No. 1, pp. 32–40, January 1991.

[3] M. Nekili and Y. Savaria, "Optimal Methods of Driving Interconnections in VLSI Circuits," *Proceedings of the IEEE International Symposium on Circuits and Systems*, pp. 21–23, May 1992.

[4] C. Y. Wu and M. Shiau, "Delay Models and Speed Improvement Techniques for RC Tree Interconnections Among Small-Geometry CMOS Inverters," *IEEE Journal of Solid-State Circuits*, Vol. SC-25, No. 5, pp. 1247–1256, October 1990.

[5] L. Bisdounis, S. Nikolaidis, O. Koufopavlou, and C. E. Goutis, "Modeling the CMOS Short-Circuit Power Dissipation," *Proceedings of the IEEE International Symposium on Circuits and Systems*, pp. 4.469–4.472, May 1996.

[6] A. M. Hill and S.-M. Kang, "Statistical Estimationof Short-Circuit Power in VLSI Circuits," *Proceedings of the IEEE International Symposium on Circuits and Systems*, pp. 4.105–4.108, May 1996.

[7] A. Hirata, H. Onodera, and K. Tamaru, "Estimation of Short-Circuit Power Dissipation and Its Influence on Propagation Delay for Static CMOS Gates," *Proceedings of the IEEE International Symposium on Circuits and Systems*, pp. 4.751–4.754, May 1996.

[8] V. Adler and E. G. Friedman, "Delay and Power Expressions for a CMOS Inverter Driving a Resistive-Capacitive Load," *Proceedings of the IEEE International Symposium on Circuits and Systems*, pp. 4.101–4.104, May 1996.

[9] A. I. Kayssi, K. A. Sakallah, and T. M. Burks, "Analytical Transient Response of CMOS Inverters," *IEEE Transactions on Circuits and Systems I: Fundamental Theory and Applications*, Vol. CAS I-39, No. 1, pp. 42–45, January 1992.

[10] T. Sakurai and A. R. Newton, "Alpha-Power Law MOSFET Model and its Applications to CMOS Inverter Delay and Other Formulas," *IEEE Journal of Solid-State Circuits*, Vol. SC-25, No. 2, pp. 584–594, April 1990.

[11] H. Shichman and D. A. Hodges, "Modeling and Simulation of Insulated-Gate Field-Effect Transistor Switching Circuits," *IEEE Journal of Solid-State Circuits*, Vol. SC-3, No. 3, pp. 285–289, September 1968.

[12] H. J. M. Veendrick, "Short-Circuit Dissipation of Static CMOS Circuitry and Its Impact on the Design of Buffer Circuits," *IEEE Journal of Solid-State Circuits*, Vol. SC-19, No. 4, pp. 468–473, August 1984.

[13] S. R. Vemuru and N. Scheinberg, "Short-Circuit Power Dissipation Estimation for CMOS Logic Gates," *IEEE Transactions on Circuits and Systems I: Fundamental Theory and Applications*, Vol. CAS I-41, No. 11, pp. 762–766, November 1994.